



# Glacier Clusters identification across Chilean Andes using Topo-Climatic variables

Identificación de clústeres glaciares a lo largo de los Andes chilenos usando variables topoclimáticas

## Historial del artículo

### Recibido:

15 de octubre de 2020

### Revisado

30 de octubre de 2020

### Aceptado:

05 de noviembre de 2020

Alexis Caro<sup>a</sup>; Fernando Gimeno<sup>b</sup>; Antoine Rabatel<sup>a</sup>; Thomas Condom<sup>a</sup>; Jean Carlos Ruiz<sup>c</sup>

<sup>a</sup> Université Grenoble Alpes, CNRS, IRD, Grenoble-INP, Institut des Géosciences de l'Environnement (UMR 5001), Grenoble, France.

<sup>b</sup> Department of Environmental Science and Renewable Natural Resources, University of Chile, Santiago, Chile.

<sup>c</sup> Sorbonne Université, Paris, France.

## Keywords

Chilean Andes, climatology, glacier clusters, topography

## Abstract

Using topographic and climatic variables, we present glacier clusters in the Chilean Andes (17.6-55.4°S), where the Partitioning Around Medoids (PAM) unsupervised machine learning algorithm was utilized. The results classified 23,974 glaciers inside thirteen clusters, which show specific conditions in terms of annual and monthly amounts of precipitation, temperature, and solar radiation. In the Dry Andes, the mean annual values of the five glacier clusters (C1-C5) display precipitation and temperature difference until 400 mm (29 and 33°S) and 8°C (33°S), with mean elevation contrast of 1800 m between glaciers in C1 and C5 clusters (18 to 34°S). While in the Wet Andes the highest differences were observed at the Southern Patagonia Icefield latitude (50°S), where the mean annual values for precipitation and temperature show maritime precipitation above 3700 mm/yr (C12), where the wet Western air plays a key role, and below 1000 mm/yr in the east of Southern Patagonia Icefield (C10), with differences temperature near of 4°C and mean elevation contrast of 500 m. This classification confirms that Chilean glaciers cannot be grouped only latitudinally, hence contributing to a better understanding of recent glacier volume changes at a regional scale.

## Palabras clave

Andes chilenos, clústeres glaciares, climatología, topografía.

## Resumen

Utilizando variables topográficas y climáticas, presentamos clústeres glaciares en los Andes chilenos (17.6-55.4°S), donde se ejecutó el algoritmo de aprendizaje automático no supervisado Partitioning Around Medoids (PAM). Los resultados clasificaron 23,974 glaciares dentro de trece clústeres, que muestran condiciones específicas en términos de cantidades anuales y mensuales de precipitación, temperatura y radiación solar. En los Andes secos, los valores medios anuales de cinco clústeres glaciares (C1-C5) muestran una diferencia de precipitación y temperatura de hasta 400 mm (29 y 33°S) y 8°C (33°S), con una resta de elevación promedio de 1800 m entre glaciares clústeres C1 y C5 (18 a 34°S). Mientras que en los Andes húmedos las mayores diferencias se observaron en la latitud del Campo de Hielo Patagónico Sur (50°S), donde los valores medios anuales de precipitación y temperatura muestran una precipitación marítima por encima de 3700 mm/año (C12), donde el aire húmedo occidental juega un papel importante, y por debajo de 1000 mm/año al este del Campo de Hielo Patagónico Sur (C10), con diferencias de temperatura cercanas a 4°C y una resta de elevación promedio de 500 m. Esta clasificación confirma que los glaciares chilenos no pueden agruparse solo latitudinalmente, contribuyendo a una mejor comprensión de los cambios recientes en el volumen de los glaciares a escala regional.

## Introduction

The glacier behaviours are linked to the regional climate variability (Braithwaite & Hughes, 2020; Fujita & Ageta, 2000; Gerbaux et al., 2005; Huss & Fischer, 2016; Ohmura et al., 1992; Sakai & Fujita, 2017), showing in wetter conditions to be more sensitive to atmospheric warming than those found in dry regions (Ohmura et al., 1992; Radić & Hock, 2011). Conversely, glaciers located in arid regions are more sensitive to precipitation fluctuations (Fujita, 2008; Kinnard et al., 2020). However, it was observed that glacier behaviours not only respond to the climatic variability; for instance, exposure of the glacier and geometry (e.g. slope, hypsometry) proved to be relevant to explain glacier behaviours (Rabatel et al., 2013). In the Alps and Asia this relationship between topo-climatic and glacier behaviours was observed, where the temperature and precipitation were the most important predictors of the glacier area variation and its mass balance (Abermann et al., 2011; Bolibar et al., 2020; Davaze et al., 2020; Liu et al., 2016; Wang et al., 2019), explaining up to 79% of the glacier mass balances variance (Bolibar et al., 2020). On the other hand, the glacier slopes and elevations explained the 36% of the variance in this region (Davaze et al., 2020).

In the Andes, the glaciers cover a broad range of latitudes and elevations, showing an accelerated shrinkage from mid-20th century in Chile (e.g. Bown et al., 2008, 2013; Farías-Barahona et al., 2020a; Malmros et al., 2016; Masiokas et al., 2020; Meier et al., 2018; Rabatel et al., 2011; Rivera et al., 2000, 2012; Rivera & Bown, 2013; Seehaus et al., 2019). In the Extratropical Andes in Chile, the glacier mass lost was explained mostly by climatic variables like precipitation, temperature, and solar radiation (Ayala et al., 2016; Falaschi et al., 2019; Kinnard et al., 2020; Macdonell et al., 2013; Masiokas et al., 2016; Rabatel et al., 2011; Ragetti & Pellicciotti, 2012; Schaefer et al., 2017; Weidemann et al., 2018). In turn, these variables have been fundamental to know the glacier runoff contribution in central Chile watersheds (Ayala et al., 2020; Bravo et al., 2017; Burger et al., 2019; Shaw et al., 2020). On the other hand, topographic variables of glaciers showed to be relevant in the glacier behaviours across the Andes (Fuchs et al., 2016; Rivera et al., 2005; Seehaus et al., 2019), but have not been quantitatively associated with the glacier behaviours in Chile.

In this context, the glacier topo-climatic characteristics (i.e. topographic and climatological variables) have not been studied across the Chilean Andes considering its high heterogeneity (Barcaza et al., 2017; Lliboutry,

1998; Masiokas et al., 2009; Sagredo & Lowell, 2012). Indeed, two main zones, the Dry and Wet Andes (with a limit between 35-36°S) have been considered, identifying between four to seven zones with glaciological similarities where their limits do not coincide and respond to latitudinal ranges across Chile (Barcaza et al., 2017; Dussailant et al., 2019; Lliboutry, 1998; Masiokas et al., 2009; Sagredo & Lowell, 2012). In addition, the study that considers the largest number of glaciers does not exceed 234 glacier bodies along the 4000 km considering that only Chile have near of 24,000 glaciers identified (DGA, 2015a; Sagredo & Lowell, 2012). An identification of glaciers with topo-climatic similarities could contribute to understanding the mass losses observed at a regional scale, as it has been observed in the reference glacier Echaurren Norte (ECH; 33.6°S, 70.1°W) in Central Chile, which has the longest time series of mass balance records in the Southern Hemisphere (DGA, 2009; Masiokas et al., 2016; Peña et al., 1987; Zemp et al., 2019). However, its negative mass balance from 1955 is greater compared with other glaciers of the same watershed (Ayala et al., 2020; Farías-Barahona et al., 2019, 2020b).

In order to identify the glacier similarities, we present a glacier cluster classification across the Chilean Andes using topo-climatic variables from the glacier national inventory of Chile and TerraClimate datasets, for 23,974 glaciers during the period 1980-2019 (Abatzoglou et al., 2018; DGA, 2015a). Goal in which the gridded data allows documenting the climate in poorly monitored regions (Condom et al., 2020; Manz et al., 2016; Schumacher et al., 2020). These glacier clusters will be calculated using the Partitioning Around Medoids (PAM) algorithm (Kaufman & Rousseeuw, 2008) and will allow identifying representative glaciers of zones with topo-climatic similarities.

## Materials and methods

### a) Topographic variables from the GNI of Chile

The location and topographical characteristics of the Chilean glaciers were obtained from the Glacier National Inventory version 2015 (GNI), available from the Dirección General de Aguas of Chile (DGA, 2015a). For the western side of the Andes in the latitude range 17.6-55.4°S, this inventory presents higher accuracy compared to global inventories such as the Randolph Glacier Inventory v6.0 (RGI Consortium, 2017). From the GNI we identified 23,974 glacier bodies, with a total surface area of 22,130 km<sup>2</sup>. The GNI provides eight topographic variables such as area (km<sup>2</sup>), elevation (mean, maximum, minimum),

aspect, slope, latitude and longitude. We selected four topographic variables to estimate glacier clusters: elevation (mean, maximum, minimum) and aspect (four variables).

#### b) Climate variables from the TerraClimate dataset

The climatic variables were extracted from the TerraClimate (TC) product. TC comprises a global climate dataset based on reanalysis data since 1958, with a 4 km grid size of spatial resolution at monthly time series. This dataset was validated with the Global Historical Climatology Network using 3,230 stations for temperature ( $r = 0.95$ ; MAE  $0.32^{\circ}\text{C}$ ) and 6,102 stations for precipitation ( $r = 0.90$ ; MAE 9.1%) (Abatzoglou et al., 2018). The variables such as mean, maximum, minimum temperatures, precipitation and solar radiation were processed. From these five variables, we calculated annual (five variables) and monthly (sixty variables) values for the period 1980-2019, obtained sixty-five climate variables in total. The annual values were estimated considering the mean of the annual sum (precipitation) or the mean of the annual mean (temperature and solar radiation), while the monthly values were calculated with the monthly mean in forty years. Regarding to the mean temperature, this was estimated from the maximum and minimum monthly temperatures.

#### c) Glacier clusters analysis from the Partitioning Around Medoids (PAM) algorithm

The topographic and climatic variables were grouped to make a Topo-Climatic variables matrix (TCM). The TCM with 23,974 glacier bodies and with sixty-nine topo-climatic variables, considered all glacier types. This clustering was developed by means of the k-medoids technique using the Partitioning Around Medoids (PAM) algorithm. The PAM algorithm divides the data set into groups where each one is represented by one of the data points in the group. These points are called a medoids cluster, which is an object within a cluster for which the average difference between it and all other cluster members is minimal (Kaufman & Rousseeuw, 2008). Similar methodologies have been used previously for glaciological studies (Dowson et al., 2020; Sagredo & Lowell, 2012; Sevestre & Benn, 2015). The cluster numbers were optimized using the Silhouette method which consists in running the PAM algorithm using different cluster numbers. The PAM results and Silhouette optimisation are compared through a Principal Component Analysis (PCA) to identify dominant explanatory variables in the glacier clusters. (Maćkiewicz & Ratajczak, 1993; Sagredo & Lowell, 2012).

## Results

The 23,984 glaciers found across the Chilean Andes ( $17.6$  to  $55.4^{\circ}\text{S}$ ) show great differences regarding climatic and topographic variables. Figure 1 displays, from north to south, an increase in mean annual temperature and mean annual total precipitation, which is associated with a decrease in elevation and an increase in the total glacier surface area. Considering the limit between the Dry and Wet Andes at  $35^{\circ}\text{S}$  (Lliboutry, 1998), the north shows colder and drier conditions (annual for average in  $T < 4^{\circ}\text{C}$  and  $P < 0.8$  m/yr) and above 1500 m a.s.l., with a small surface if compared to the Wet Andes which have higher temperatures and precipitations (annual for average in  $T > 4^{\circ}\text{C}$  and  $P > 0.8$  m/yr) with elevations below the 1500 m a.s.l. These topo-climatic variables among others, allowed identifying thirteen glacier clusters through the PAM method and Silhouettes cluster optimisation. The results are presented in figure 2 using Principal Components Analysis (PC). The first two PCs explain 84.1% of the variance shared between the variables (PC1 67.2%, PC2 16.6%). The Pearson linear correlation between variables in PC1 shows high adjustment of the mean elevation ( $r = -0.86$ ), followed by the maximum annual mean temperature ( $r = 0.76$ ) and maximum mean temperature of January ( $r = 0.60$ ). Topographic variables, like aspect, showed low correlation ( $r = -0.18$ ).

Regarding the glacier surface areas in the identified glacier clusters, the C1-C4 zone ( $18.1-34.2^{\circ}\text{S}$ ) presents high adjustment with respect to the precipitation (95.3%) and minimum elevation (4.7%) explaining 98% of the variance. Meanwhile, in the C6-C9 zone ( $41.9-48.2^{\circ}\text{S}$ ) the 95% of the variance is explained by the latitude (90.5%) and solar radiation (9.5%). The variance of glacier surface areas in the C11-C13 zone ( $49.2-54.6^{\circ}\text{S}$ ) can be explained by the precipitation in 99%. Between these three zones (C1-C4, C6-C9 and C11-C13), the C5 and C10 glacier clusters are considered as transition clusters, as they do not fit well within the other clusters. These thirteen glacier clusters are presented in table 1 and figure 3.

The first zone C1-C4 mainly distributed between the latitude range  $18.1-34.2^{\circ}\text{S}$  (Q1-Q3) include glaciers from the Desert Andes to part of the Central Andes, covering watersheds from the río Lluta ( $17.6^{\circ}\text{S}$ ) to río Rapel ( $34.7^{\circ}\text{S}$ ). This zone has a glacier surface area of  $976.5$  km<sup>2</sup> (3874 glacier bodies) with a mean elevation of about 4500 m a.s.l. The climate shows an annual mean temperature of  $-1.4^{\circ}\text{C}$ , an annual mean precipitation amount of 292 mm/yr and solar radiation of 207 W/m<sup>2</sup>. In the north of this zone, the C1 cluster ( $18.1-21.6^{\circ}\text{S}$ )

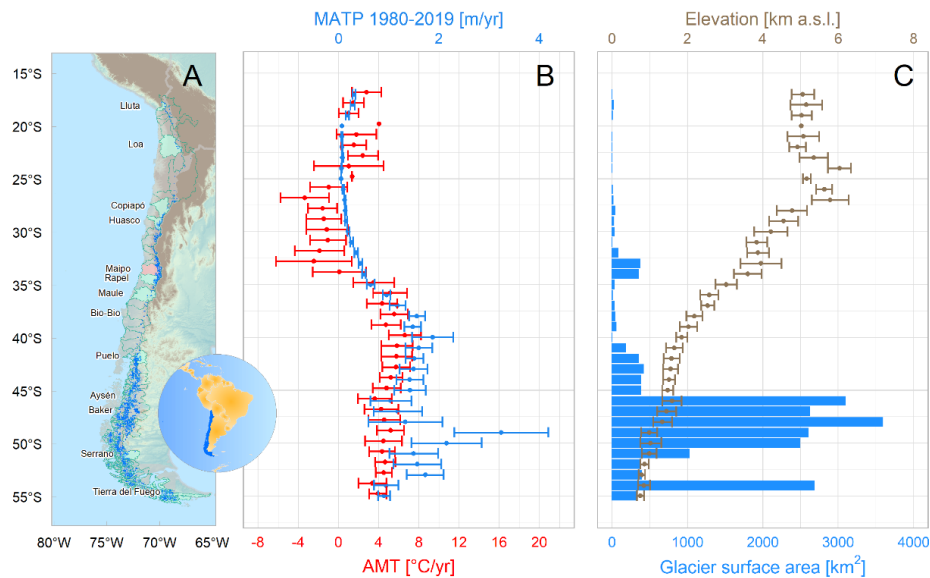


**Figure 1.** Chilean glacier locations and its topo-climatic variables distribution across the Andes. (A) The glacier distribution extracted from the Chilean GNI is presented (blue) as well the partial glacierized watersheds (green polygons), followed by (B) annual mean temperature (AMT) (red) and mean total annual precipitation (MATP) (blue) distribution between 1980-2019, and (C) the latitudinal total glacier surface area (blue bars) associated with the mean elevation (brown) observed in the Chilean Andes. *Source:* self-made.

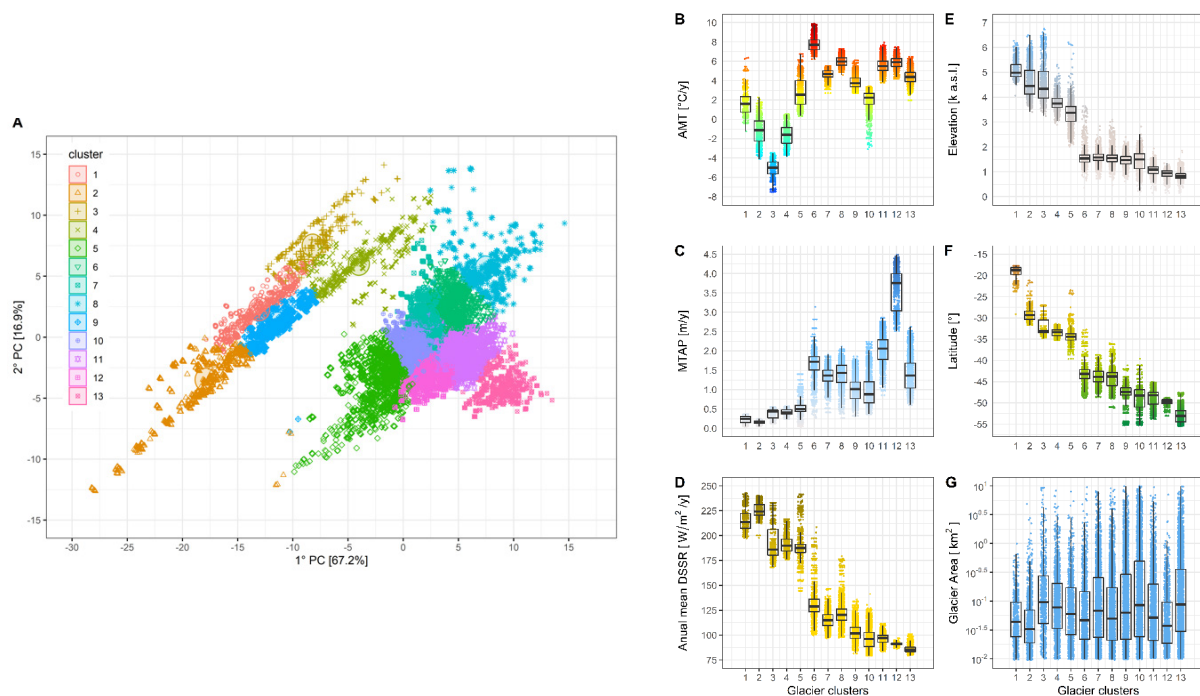


**Figure 2.** Relevance of the thirteen clusters in the first two CPs (A) and the behaviour of the climatic (B, C, D) and topographic (E, F, G) variables in each glacier cluster across Chilean Andes between 1980-2019. The annual mean temperature (AMT), mean total annual precipitation (MATP) and the annual mean downward surface shortwave radiation (DSSR) are presented. *Source:* self-made.

shows the highest glacier mean elevation (5119 m a.s.l.), the smallest glacial surface (45 km<sup>2</sup>) and the warmest climate in the C1:C4 zone (1.7°C). In the río Copiapó watershed (27.2°S), C1, C2 and C3 are overlapped. The C2 cluster (28.5-30.4°S) and C3 (32.4-33.5°S) present a similar elevation, but the glacial surface is almost five times higher in C3 (490 km<sup>2</sup>) in comparison with C2 (101 km<sup>2</sup>), and a similar situation is observed in the annual mean precipitations (382 and 158 mm/yr). The solar radiation shows a significant change from C1, C2 to C3, as well as the temperature. The C3 cluster presents the lowest annual mean temperature (-5°C) of the C1-C4 zone. C4 cluster (32.9-34.2°S) shows a total glacier surface area of 341 km<sup>2</sup> with the highest amounts of annual mean precipitation (421 mm/yr) and the lowest average elevation at 3732 m a.s.l. for this region. With respect to the monthly climatology, the annual mean precipitation in C1 is concentrated in summer (November to March), with February showing the highest amount (70 mm) and the temperature is generally above 0°C except in the winter season (June to August) with a monthly minimum of -2.5°C (July). The solar radiation shows greater values from September to March, being interrupted in February due to summer precipitations. Between C2 to C4 the winter precipitation displays higher amounts from May to August (78 mm in July for C4), but these are less relevant in C2, where the summer precipitations are more important than in C3-C4. The temperature is below 0°C between May to October in C2 and C4, while C3 has low temperatures all year long, showing the higher temperatures during summer months (December to March). The amplitude of the monthly solar radiation is similar from C2 to C4, concentrating from October to March, where the highest radiation amounts are seen in C2 (335 w/m<sup>2</sup>, December).

The C5 cluster is located in the Central Andes and Lakes District zones. C5 gathers glaciers found between latitudes 33.9-35.6°S (Q1-Q3), however, its limits extend from the río Huasco (29.1°S) to río Bio-Bio (37.5°S) watersheds and shares latitudinal range with C3 and C4 clusters. Unlike the C1-C4 zone, C5 presents a smaller glacier area than close clusters with 176 km<sup>2</sup> (969 glacier bodies) and a lower elevation (3259 m a.s.l.). On the other hand, the annual mean temperature and precipitation are higher than for all clusters to the north. At monthly scale, the highest precipitation occurs in the winter season (June, 104 mm) and the annual mean temperature reaches values below 0°C from June to September. The solar radiation is dominant from October to March, with highest value in December (297 w/m<sup>2</sup>).

The third zone comprises four glacier clusters from C6 to C9, concentrated between latitude 42-48.2°S (Q1-Q3), distributed between río Maule (36.6°S) and río Serrano (50.9°S) watersheds and covering from Lakes District to South Patagonia, with a total glacierized area of 3,336 km<sup>2</sup> (9386 glacier bodies) and an average elevation above 1535 m a.s.l. The climate is warmer and wetter than for the previously described clusters (5.7°C; 1344 mm/yr), and shows a lower level of solar radiation with an annual mean of 118 w/m<sup>2</sup>. In this zone there is an important latitudinal overlap between glacier clusters, as was seen in the zone C1-C4. The C6 cluster (42-43.8°S) contains a smaller glacier surface area (227 km<sup>2</sup>), but the greatest amounts in the climatic variables (7.9°C, 1651 mm/yr, and 133 W/m<sup>2</sup>) of the C6-C9 zone. To the south, the C7 cluster (42.3-44.9°S) gathers the second largest glacierized area with 859 km<sup>2</sup> and the highest elevation (1612 m a.s.l.) of the zone. It is followed by the C8 cluster (43.4-47.1°S) and the C9 cluster (46.4-48.2°S), which have the largest glacier area in the C6-C9 zone with 1670 km<sup>2</sup> and the lowest elevation (1450 m a.s.l.). The climate in C9 shows the lowest annual mean temperatures (3.9°C), precipitation (1026 mm) and solar radiation (103 W/m<sup>2</sup>) of this zone. From C6-C8, the monthly precipitation is concentrated in the winter season, with highest values in June where C6 has the most important monthly value (218 mm). The precipitation in C9 occurs mainly between the months of March to August, with a maximum in June (105 mm), showing lower monthly variation with respect to C6-C8. The annual mean temperature in C6 and C8 does not present values below 0°C, while C7 and C9 show monthly mean temperatures of -1°C and -1.2°C in July. The radiation decreases in winter months with lowest value in June (C9, 28 W/m<sup>2</sup>).

The C10 cluster, similarly to C5, does not have the same characteristics as the adjacent glacier clusters. C10 is located between latitudes 46.8-50.8°S (Q1-Q3) from río Puelo watershed (42.1°S) to the southern islands at Tierra del Fuego (55°S), associated with the North Patagonia and Tierra del Fuego glacier zones. It comprises the largest glacier surface area in Chile with 14031 km<sup>2</sup> (3001 glacier bodies) and an average elevation of 1462 m a.s.l. The climate shows values well below those observed in the C6-C9 zone, with which it shares a latitudinal range, and has an annual mean temperature of 2°C, an annual mean precipitation of 983 mm/yr, and an average solar radiation of 98 w/m<sup>2</sup>. This zone includes a large part of the Southern Patagonia Icefield and Cordillera Darwin. The monthly precipitation is distributed throughout the year, with mean values higher in March-April (102 mm in April) and the monthly temperature lowest value in

**Table 1**

Topo-climatic values for the thirteen glacier clusters across Chile. \* Indicates between 25 to 75% of the latitudinal concentration of glaciers.

Cluster	Latitude quartile Q1-Q3* [°S]	Mean Elevation [m a.s.l.]	Glacier Area [km <sup>2</sup> ] Total; mean	Number of glaciers	Annual mean Temperature [°C/yr] 1980-2019	Annual mean Precipitation [mm/yr] 1980-2019	Annual mean DSSR [W/m <sup>2</sup> /yr] 1980-2019
1	18.1-21.6	5119	44.7; 0.07	575	1.7	207	218
2	28.5-30.4	4578	100.7; 0.08	1151	-1.2	159	226
3	32.4-33.5	4430	490; 0.50	963	-5	382	193
4	32.9-34.2	3732	341.1; 0.28	1185	-1.2	421	191
5	33.9-35.6	3259	175.7; 0.18	969	3.1	574	188
6	42-43.8	1600	227.2; 0.20	1097	7.9	1651	133
7	42.3-44.9	1612	858.8; 0.30	2790	4.8	1314	118
8	43.4-47.1	1480	580; 0.22	2570	6.2	1387	118
9	46.4-48.2	1450	1669.8; 0.57	2929	3.9	1026	103
10	46.8-50.8	1462	14030.5; 4.67	3001	2	983	98
11	47.8-51.2	1009	939; 0.34	2764	5.4	2044	94
12	49.2-49.8	909	108.1; 0.10	1013	5.9	3737	91
13	51.9-54.7	852	2602.7; 0.87	2977	4.1	1341	86

Source: self-made.

July (-2.5°C), with monthly values below 0°C from May to September, and a maximum value in January (6.7°C). The radiation presents a maximum in January (174 W/m<sup>2</sup>) and a lowest value in June (26 W/m<sup>2</sup>).

The fifth and southernmost zone, C11:C13 is located between latitude range 49.2.-54.7°S (Q1-Q3) across Aysén fiord (45.1°S) to southern islands of Tierra del Fuego (55°S). It is highly overlapped to C10, and gathers a glacierized surface area of 3,650 km<sup>2</sup> (6754 glacier bodies) with a mean elevation above 924 m a.s.l. The annual mean temperature is 5.2°C, while annual mean precipitation is the highest of the five studied zones (2374 mm/yr), presenting the low solar radiation (90 w/m<sup>2</sup>). In this zone, a strong longitudinal distribution is identified from west (coast) to east (Patagonia) of the mountain range, where C12 glacier cluster (49.2-49.8°S) is located between coastal islands (48.8°S) and islands south of the Estrecho de Magallanes (53.8°S) with the lower glacierized area (108 km<sup>2</sup>) and the highest annual mean temperature (5.9°S) of the zone. Precipitation of 3,737 mm/yr is the highest amount observed in the thirteen glacier clusters studied. To the east of C12, the C11 cluster (47.8-51.2°S) is distributed between the coastal islands at the río Aysén watershed (45.7°S) and islands to the south of the Estrecho de Magallanes (53.8°S). The glacierized surface area in

C11 is 939 km<sup>2</sup> and presents the highest elevation (1,009 m a.s.l.) of the zone C11:C13, while the annual mean precipitation is the second highest amount after C12 with 2044 mm/yr. The last glacier cluster, C13 (51.9-54.7°S) is located between the río Baker watershed (47.4°S) and islands to the south of the Beagle Channel (55.4°S). This glacier cluster has the largest glacierized surface area (2,603 km<sup>2</sup>) and lowest elevation (852 m a.s.l.) in the zone, as well as the lowest annual mean temperature (4.1°C), precipitation (1341 mm/yr) and solar radiation (86 W/m<sup>2</sup>). The precipitation is well distributed along the year, showing highest values in March or April (372 mm in March for C12), and the smallest values in September. In this zone the temperature presents a lower amplitude than other zones and the monthly mean is never 0°C. C13 has the lowest radiation value of all clusters with 19 W/m<sup>2</sup> in June.

## Discussion

In this section we first discuss the results of the thirteen glacier clusters regarding the six glaciological zones currently used to describe the glacier distribution in Chile. Then, we present the benefits in identifying glacier clusters with similar topo-climatic conditions.

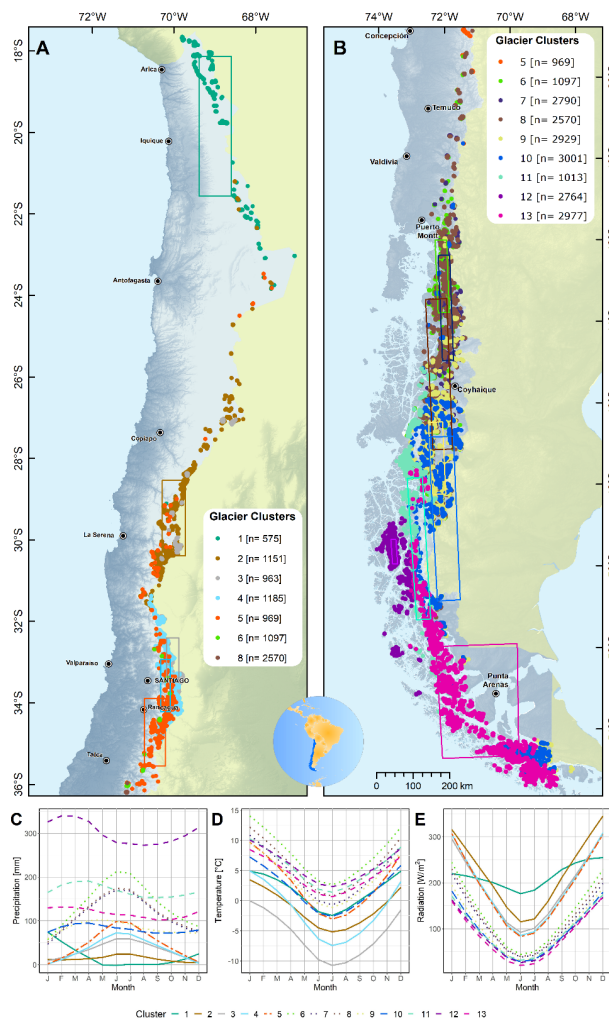


**Figure 3.** Glacier clustering distribution in Chile and climograms. The Chilean glacier's location is associated with a cluster through points (color palette), where the concentration in latitude and longitude ranges (Q1-Q3) of these is represented by rectangles (A). The three plots below show from left to right the average monthly distribution precipitation, temperature and solar radiation associated with each cluster. *Source:* self-made.

#### a) Performance of the glacier clustering regarding climate conditions across the Andes

The thirteen glacier clusters identified in our study have latitudinal and longitudinal overlaps, which are however limited for C1 (north) and C12 (west of the Patagonian icefields). The most important number of glacier bodies associated with the latitude quartiles (between 25 and 75%) for each glacier cluster, allows identifying a glacier latitudinal distribution with topo-climatic similarities and without overlap to the north of the 31°S. This was used in previous studies to define the glaciological zones across Chile (Barcaza et al., 2017; Dussailant et al., 2019; Lliboutry, 1998; Masiokas et al., 2009; Sagredo & Lowell, 2012). But, this latitudinal

differentiation of the glacier clusters was not clear to the south of the latitude 31°S. Overall, the above mentioned studies identified between four to seven glaciological zones across Chile, even aggregated into two macro zones, the Dry and Wet Andes with a limit between 35-36°S. For instance, Lliboutry (1998) established the first identification of glacial zones in Chile, then Sagredo and Lowell (2012) identified glacial zones using climatic characteristics on a considerable number of glaciers (<234 glacier bodies); from north to south they distinguished: the Desert Andes (17 to 27-32°S), the Central Andes (27-32 to 35-36°S), the Lakes District (35-36 to 41-46°S), the North Patagonia (41-43 to 44-48°S), the South Patagonia (46-48 to 52-53°S) and the Tierra del Fuego (52-53 to -56°S).

In our analysis, for the Dry Andes, five glacier clusters are identified, C1 to C5, with the southernmost cluster observed near 37°S. Here, the Desert Andes gathers the clusters C1 and C2, a zone where Schumacher et al. (2020) observed a higher precipitation between 17-19°S (C1; 207 mm/yr) with respect to the rest of Desert Andes (C2; 159 mm/yr), with precipitation amounts between 100 and 500 mm/yr. These ranges of precipitation in C2 agree with that observed by Kinnard et al. (2020) where the Guanaco glacier mass balance is mostly sensitive to precipitation variations, with precipitation amounts near the glacier between 170 and 240 mm/yr (81% occurring in winter). Glacier clusters C3 to C5 (32.4-35.5°S) are found in the Central Andes, showing a specific elevation distribution with an important precipitation seasonality concentrated during the winter, with higher amounts than observed by Sagredo and Lowell (2012). In this zone, Schumacher et al. (2020) identified a high heterogeneity in the weather records between 30-35°S below 3200 m a.s.l., where C5 (3.1°C; 3259 m a.s.l.) is warmer and wetter with respect to C3 and C4. C3 and C4 clusters showed annual mean temperatures less in C3 with similar precipitation. Measurements on the Bello (C3) and Pirámide (C4) glaciers confirm this behaviour (e.g. similar accumulation amounts), and summer temperatures of -0.8°C in Bello glacier and 1.2°C in Pirámide glacier (DGA, 2015b).

In the Wet Andes, eight glacier clusters are identified (C6 to C13). In the northern Wet Andes, the Lakes District and Northern Patagonia cover a high latitudinal range between 35-36°S and 41-46°S, with the Lakes District being considered up to 41°S. In the Lakes District, six widespread glacier clusters from C5 to C10 can be found. They show a high climatic heterogeneity, with average precipitation (temperature) ranges between 574 mm/yr (3.1°C) in the north to 1651 mm/yr (7.9°C) in the south, accompanied by a decrease in elevation. South from 41°S to 52-53°S in the Patagonian zone and south of 53°S in the Tierra del Fuego, the glaciers show high topo-climatic differences. Studies across the Northern Patagonia Icefield (NPI) and Southern Patagonia Icefield (SPI) observed a large difference in precipitation between the west and the east (Bravo et al., 2019; Warren, 1993), with the San Rafael and San Quintin glaciers variations, to the west to NPI, mainly controlled by changes in winter precipitation (Bertrand et al., 2012; Warren, 1993; Winchester & Harrison, 1996). In the NPI, Barcaza et al. (2017) observed a large difference between records of weather stations located to the west of the NPI compared to those located to the east, where Laguna San Rafael station (46.6°S, 73.9°W; 0 m a.s.l.), in the west, showed warmer and wetter conditions (6.9°C; 3144 mm/yr) than Lago Colonia station (47.3°S, 73.1°W; 150 m a.s.l.), located to the east (4.9°C; 1649 mm/yr). The same

behavior was identified for the C12 cluster extended to the west of the NPI (5.4°C; 2004 mm/yr) and C9 to the east (3.9°C; 1026 mm/yr). High precipitation amounts to the west are likely due to the control by the wet Western air masses from the Pacific Ocean (Langhamer et al., 2018; Warren, 1993). For this latitude range Sagredo and Lowell (2012) identified homogeneous precipitations throughout the year with maximum in summer to the south of 48°S, however Bravo et al. (2019) identified solid precipitation concentrated in winter for NPI and to the west of the SPI. On the other hand, to the east of the SPI the precipitation is homogeneous throughout the year.

#### b) Implications for the Chilean glaciers monitoring

To understand the glacier response to changes in climate conditions, it is essential to better understand the climate-glaciers relationships. Several studies already focussed on these aspects in the Southern Andes, particularly across the Chilean Andes (Ayala et al., 2016; Ayala et al., 2020; Bravo et al., 2017; Burger et al., 2019; Macdonell et al., 2013; Masiokas et al., 2016; Ragettli et al., 2013; Schaefer et al., 2020). Recently, Schaefer et al. (2020) estimated the energy balance in Bello (33°S), Mocho-Choshuenco (39.5°S) and Tyndall (51°S) glaciers, showing a decrease in the solar radiation importance on the melting processes from north to south, increasing the relevance of the sensible heat fluxes, for which the air temperature is very important. Decrease in solar radiation was observed in our glacier clusters analysis, with solar radiation decreasing from 198 W/m<sup>2</sup> (Bello glacier) to 95 W/m<sup>2</sup> (Tyndall glacier), and the highest temperatures and precipitation occurring in the Mocho-Choshuenco glacier (7.1°C; 1732 mm/yr), followed by the Tyndall glacier (3.2°C; 1345 mm/yr), and the coldest and driest being Bello glacier (-3.0; 420 mm/yr). Similarly, the Echaurren Norte glacier (33.6°S, 70.1°W) in Central Chile, considered as a reference glacier due to its long time series of mass balance records in the Southern Hemisphere since 1976 (DGA, 2009; Masiokas et al., 2016; Peña et al., 1987; Zemp et al., 2019), has shown a negative accumulated mass balance from 1955. However, this mass loss appears to be larger than other glaciers in the same watershed (Ayala et al., 2020; Fariás-Barahona et al., 2019, 2020b).

In addition, it has been shown that 78% of the Echaurren glacier mass balance variance was explained by precipitation variability followed by the temperature (Masiokas et al., 2016). Considering the results of our clustering analysis, the most important mass loss experienced by the Echaurren Norte glacier with regards to the neighbouring glaciers could be explained by the heterogeneity in climate conditions

encountered inside the Maipo watershed (Ayala et al., 2020). In our analysis, the glaciers within the Maipo watershed are distributed between different clusters (C3, C4, and C5), exhibit high precipitation and temperature differences. The C3 glacier cluster with the most important glacierized surface area (64%) displays an annual mean temperature (precipitation) of  $-5^{\circ}\text{C}$  (382 mm/yr), followed by C4 that gathers 31% of the glacierized surface area of the Maipo watershed. The 3rd cluster (C5) shows a lower glacierized surface area (5%) but presents the warmer and wetter climate conditions ( $3.1^{\circ}\text{C}$ , 574 mm/yr). It is precisely in the C5 cluster where the Echaurren Norte glacier is located. On the other hand, C5 cluster (3259 m a.s.l.) shows the most important surface area of rock glaciers in the Maipo watershed (68%).

## Conclusions

The use of topo-climatic variables from 23,974 glaciers in the Chilean Andes ( $17.6\text{--}55.4^{\circ}\text{S}$ ) allowed the identification of thirteen glacier clusters with a particular climatology, where annual mean temperature, precipitation and solar radiation show variations from north to south and diverse annual regimes.

This new classification of glacierized zones in Chile, using the globally validated TerraClimate product and compared with national studies, demonstrated that a latitudinally based classification made on the basis of a few glaciers is not representative of the Chilean glaciers, due to an observed high latitudinal overlap of climate regimes. For instance, the Central Andes presented various glacier clusters associated with the elevation, meanwhile, the Patagonian glaciers showed longitudinally distributed glacier clusters, where the wet Western air plays a key role in the maritime to continental precipitation regimes.

Finally, the identification of these glacier clusters will contribute regionally to understand the distribution of the dominant meteorological forcing in the glacier mass balance, where the monitored glaciers could be associated with others found in the same glacier cluster, contrary to what was observed in the Echaurren Norte glacier which presents low representativeness in the Maipo watershed and consequently, this better understanding will be useful for hydrological studies in glaciated watersheds.

## Acknowledgments

We thank the Dirección General de Aguas de Chile for providing the glacier national inventory version 2015. The

TerraClimate products were obtained freely at <http://www.climatologylab.org/terraclimate.html>. This work was funded by the National Agency for Research and Development (ANID)/ Scholarship Program/ DOCTORADO BECAS CHILE/2019 – 72200174 and the Secretaría Nacional de Educación Superior, Ciencia, Tecnología e Innovación, SENESCYT/ PhD scholarship. This study was conducted in the framework of the International Joint Laboratory GREAT-ICE, a joint initiative of the IRD and universities and institutions in Bolivia, Peru, Ecuador, and Colombia.

## References

- Abatzoglou, J. T., Dobrowski, S. Z., Parks, S. A., & Hegewisch, K. C. (2018). TerraClimate, a high-resolution global dataset of monthly climate and climatic water balance from 1958-2015. *Scientific Data*, 5, 1–12. <https://doi.org/10.1038/sdata.2017.191>
- Abermann, J., Kuhn, M., & Fischer, A. (2011). A reconstruction of annual mass balances of Austria's glaciers from 1969 to 1998. *Annals of Glaciology*, 52(59), 127–134. <https://doi.org/10.3189/172756411799096259>
- Ayala, Á., Fariás-Barahona, D., Huss, M., Pellicciotti, F., McPhee, J., & Farinotti, D. (2020). Glacier runoff variations since 1955 in the Maipo River Basin, semiarid Andes of central Chile. *The Cryosphere Discussions*, 1–39. <https://doi.org/10.5194/tc-2019-233>
- Ayala, A., Pellicciotti, F., MacDonell, S., McPhee, J., Vivero, S., Campos, C., & Egli, P. (2016). Modelling the hydrological response of debris-free and debris-covered glaciers to present climatic conditions in the semiarid Andes of central Chile. *Hydrological Processes*, 30(22), 4036–4058. <https://doi.org/10.1002/hyp.10971>
- Ayala, A., Pellicciotti, F., Peleg, N., & Burlando, P. (2017). Melt and surface sublimation across a glacier in a dry environment: Distributed energy-balance modelling of Juncal Norte Glacier, Chile. *Journal of Glaciology*, 63(241), 803–822. <https://doi.org/10.1017/jog.2017.46>
- Barcaza, G., Nussbaumer, S. U., Tapia, G., Valdés, J., García, J. L., Videla, Y., Albornoz, A., & Arias, V. (2017). Glacier inventory and recent glacier variations in the Andes of Chile, South America. *Annals of Glaciology*, 58(75), 166–180. <https://doi.org/10.1017/aog.2017.28>

- Bertrand, S., Huguen, K. A., Lamy, F., Stuut, J. B. W., Torrejón, F., & Lange, C. B. (2012). Precipitation as the main driver of Neoglacial fluctuations of Gualas glacier, Northern Patagonian Icefield. *Climate of the Past*, 8(2), 519–534. <https://doi.org/10.5194/cp-8-519-2012>
- Bolibar, J., Rabatel, A., Gouttevin, I., Galiez, C., Condom, T., & Sauquet, E. (2020). Deep learning applied to glacier evolution modelling. *Cryosphere*, 14(2), 565–584. <https://doi.org/10.5194/tc-14-565-2020>
- Bown, F., Rivera, A., & Acuña, C. (2008). Recent glacier variations at the Aconcagua basin, central Chilean Andes. *Annals of Glaciology*, 48, 43–48. <https://doi.org/10.3189/172756408784700572>
- Bown, F., Rivera, A., Zenteno, P., Bravo, C., & Cawkwell, F. (2013). First glacier inventory and recent glacier variation on Isla Grande de Tierra del Fuego and adjacent islands in Southern Chile. In *Global Land Ice Measurements from Space* (pp. 661–674).
- Braithwaite, R. J., & Hughes, P. D. (2020). Regional Geography of Glacier Mass Balance Variability Over Seven Decades 1946–2015. *Frontiers in Earth Science*, 8, 1–14. <https://doi.org/10.3389/feart.2020.00302>
- Bravo, C., Bozkurt, D., Gonzalez-Reyes, Á., Quincey, D. J., Ross, A. N., Farías-Barahona, D., & Rojas, M. (2019). Assessing snow accumulation patterns and changes on the Patagonian Icefields. *Frontiers in Environmental Science*, 7, 1–18. <https://doi.org/10.3389/fenvs.2019.00030>
- Bravo, C., Loriaux, T., Rivera, A., & Brock, B. W. (2017). Assessing glacier melt contribution to streamflow at Universidad Glacier, central Andes of Chile. *Hydrology and Earth System Sciences*, 21(7), 3249–3266. <https://doi.org/10.5194/hess-21-3249-2017>
- Burger, F., Ayala, A., Farias, D., Shaw, T. E., MacDonell, S., Brock, B., McPhee, J., & Pellicciotti, F. (2019). Interannual variability in glacier contribution to runoff from a high-elevation Andean catchment: understanding the role of debris cover in glacier hydrology. *Hydrological Processes*, 33(2), 214–229. <https://doi.org/10.1002/hyp.13354>
- Condom, T., Martínez, R., Pabón, J. D., Costa, F., Pineda, L., Nieto, J. J., López, F., & Villacis, M. (2020). Climatological and Hydrological Observations for the South American Andes: In situ Stations, Satellite, and Reanalysis Data Sets. *Frontiers in Earth Science*, 8. <https://doi.org/10.3389/feart.2020.00092>
- Davaze, L., Rabatel, A., Dufour, A., Hugonnet, R., & Arnaud, Y. (2020). Region-Wide Annual Glacier Surface Mass Balance for the European Alps From 2000 to 2016. *Frontiers in Earth Science*, 8, 1–14. <https://doi.org/10.3389/feart.2020.00149>
- DGA. (2009). *Estrategia Nacional de Glaciares*. Valdivia: Technical report: Centro de Estudios Científicos (CECs).
- DGA. (2015a). *Inventario Público de Glaciares de Chile*. Santiago: Technical report: Dirección General de Aguas.
- DGA. (2015b). *Modelación de balance de masa y descargas de aguas en glaciares del Norte Chico y Chile Central* (Issue 10945). La Serena: Technical report: Centro de Estudios Avanzados de Zonas Áridas (CEAZA).
- Dowson, A. J., Sirguey, P., & Cullen, N. J. (2020). Variability in glacier albedo and links to annual mass balance for the gardens of Eden and Allah, Southern Alps, New Zealand. *The Cryosphere*, 14(10), 3425–3448. <https://doi.org/10.5194/tc-14-3425-2020>
- Dussailant, I., Berthier, E., Brun, F., Masiokas, M., Hugonnet, R., Favier, V., Rabatel, A., Pitte, P., & Ruiz, L. (2019). Two decades of glacier mass loss along the Andes. *Nature Geoscience*, 12(10), 802–808. <https://doi.org/10.1038/s41561-019-0432-5>
- Falaschi, D., Lenzano, M. G., Villalba, R., Bolch, T., Rivera, A., & Lo Vecchio, A. (2019). Six Decades (1958–2018) of Geodetic Glacier Mass Balance in Monte San Lorenzo, Patagonian Andes. *Frontiers in Earth Science*, 7. <https://doi.org/10.3389/feart.2019.00326>
- Farías-Barahona, D., Ayala, Á., Bravo, C., Vivero, S., Seehaus, T., Vijay, S., Schaefer, M., Buglio, F., Casassa, G., & Braun, M. H. (2020). 60 years of glacier elevation and mass changes in the Maipo River Basin, central Andes of Chile. *Remote Sensing*, 12(10), 1–19. <https://doi.org/10.3390/rs12101658>

- Farías-Barahona, D., Vivero, S., Casassa, G., Schaefer, M., Burger, F., Seehaus, T., Iribarren-Anaconda, P., Escobar, F., & Braun, M. H. (2019). Geodetic mass balances and area changes of Echaurren Norte Glacier (Central Andes, Chile) between 1955 and 2015. *Remote Sensing*, 11(3). <https://doi.org/10.3390/rs11030260>
- Farías-Barahona, D., Wilson, R., Bravo, C., Vivero, S., Caro, A., Shaw, T. E., Casassa, G., Ayala, Á., Mejías, A., Harrison, S., Glasser, N. F., McPhee, J., Wünderlich, O., & Braun, M. H. (2020). A near 90-year record of the evolution of El Morado Glacier and its proglacial lake, Central Chilean Andes. *Journal of Glaciology*, 66(259), 846–860. <https://doi.org/10.1017/jog.2020.52>
- Fuchs, P., Asaoka, Y., & Kazama, S. (2016). Modelling melt, runoff, and mass balance of a tropical glacier in the Bolivian Andes using an enhanced temperature-index model. *Hydrological Research Letters*, 10(2), 51–59. <https://doi.org/10.3178/hrl.10.51>
- Fujita, K. (2008). Influence of precipitation seasonality on glacier mass balance and its sensitivity to climate change. *Annals of Glaciology*, 48, 88–92. <https://doi.org/10.3189/172756408784700824>
- Fujita, K., & Ageta, Y. (2000). Effect of summer accumulation on glacier mass balance on the Tibetan Plateau revealed by mass-balance model. *Journal of Glaciology*, 46(153), 244–252. <https://doi.org/10.3189/172756500781832945>
- Gerbaux, M., Genthon, C., Etchevers, P., Vincent, C., & Dedieu, J. P. (2005). Surface mass balance of glaciers in the French Alps: Distributed modeling and sensitivity to climate change. *Journal of Glaciology*, 51(175), 561–572. <https://doi.org/10.3189/172756505781829133>
- Huss, M., & Fischer, M. (2016). Sensitivity of very small glaciers in the swiss alps to future climate change. *Frontiers in Earth Science*, 4, 1–17. <https://doi.org/10.3389/feart.2016.00034>
- Kaufman, L. & Rousseeuw, P. J. (2008). Partitioning Around Medoids (Program PAM). In L. Kaufman & P. J. Rousseeuw (Eds.), *In Finding Groups in Data* (pp. 68–125). <https://doi.org/doi:10.1002/9780470316801.ch2>
- Kinnard, C., Ginot, P., Surazakov, A., MacDonell, S., Nicholson, L., Patris, N., Rabatel, A., Rivera, A., & Squeo, F. A. (2020). Mass Balance and Climate History of a High-Altitude Glacier, Desert Andes of Chile. *Frontiers in Earth Science*, 8, 1–20. <https://doi.org/10.3389/feart.2020.00040>
- Langhamer, L., Sauter, T., & Mayr, G. J. (2018). Lagrangian Detection of Moisture Sources for the Southern Patagonia Icefield (1979–2017). *Frontiers in Earth Science*, 6, 1–17. <https://doi.org/10.3389/feart.2018.00219>
- Liu, L., Jiang, L., Sun, Y., Wang, H., Yi, C., & Hsu, H. (2016). Morphometric controls on glacier mass balance of the puruogangri ice field, central tibetan plateau. *Water (Switzerland)*, 8(11), 1–18. <https://doi.org/10.3390/w8110496>
- Lliboutry, L. (1998). Glaciers of Chile and Argentina. In J. Williams, Richard & Ferrigno (Ed.), *Satellite Image Atlas of Glaciers of the World; SOUTH AMERICA* (1st ed., pp. 109–206).
- Macdonell, S., Kinnard, C., Mölg, T., Nicholson, L., & Abermann, J. (2013). Meteorological drivers of ablation processes on a cold glacier in the semi-arid Andes of Chile. *Cryosphere*, 7(5), 1513–1526. <https://doi.org/10.5194/tc-7-1513-2013>
- Maćkiewicz, A., & Ratajczak, W. (1993). Principal Components Analysis ( PCA )\*. *Computers & Geosciences*, 19(3), 303–342. [https://doi.org/10.1016/0098-3004\(93\)90090-R](https://doi.org/10.1016/0098-3004(93)90090-R)
- Malmros, J. K., Mernild, S. H., Wilson, R., Yde, J. C., & Fensholt, R. (2016). Glacier area changes in the central Chilean and Argentinean Andes 1955–2013/14. *Journal of Glaciology*, 62(232), 391–401. <https://doi.org/10.1017/jog.2016.43>
- Manz, B., Buytaert, W., Zulkafli, Z., Lavado, W., Willems, B., Robles, L. A., & Rodríguez-Sánchez, J. P. (2016). High-resolution satellite-gauge merged precipitation climatologies of the tropical andes. *Journal of Geophysical Research*, 121(3), 1190–1207. <https://doi.org/10.1002/2015JD023788>
- Masiokas, M. H., Christie, D. A., Le Quesne, C., Pitte, P., Ruiz, L., Villalba, R., Luckman, B. H., Berthier, E., Nussbaumer, S. U., González-Reyes, Á., McPhee,

- J., & Barcaza, G. (2016). Reconstructing the annual mass balance of the Echaurren Norte glacier (Central Andes, 33.5° S) using local and regional hydroclimatic data. *Cryosphere*, 10(2), 927–940. <https://doi.org/10.5194/tc-10-927-2016>
- Masiokas, M. H., Rabatel, A., Rivera, A., Ruiz, L., Pitte, P., Ceballos, J. L., Barcaza, G., Soruco, A., Bown, F., Berthier, E., Dussailant, I., & MacDonell, S. (2020). A Review of the Current State and Recent Changes of the Andean Cryosphere. *Frontiers in Earth Science*, 8, 1–27. <https://doi.org/10.3389/feart.2020.00099>
- Masiokas, M. H., Rivera, A., Espizua, L. E., Villalba, R., Delgado, S., & Aravena, J. C. (2009). Glacier fluctuations in extratropical South America during the past 1000 years. *Palaeogeography, Palaeoclimatology, Palaeoecology*, 281(3–4), 242–268. <https://doi.org/10.1016/j.palaeo.2009.08.006>
- Meier, W. J. H., Griesbinger, J., Hochreuther, P., & Braun, M. H. (2018). An updated multi-temporal glacier inventory for the patagonian andes with changes between the little ice age and 2016. *Frontiers in Earth Science*, 6, 62. <https://doi.org/10.3389/feart.2018.00062>
- Ohmura, A., Kasser, P., & Funk, M. (1992). Climate at the equilibrium line of glaciers. *Journal of Glaciology*, 38(130), 397–411. <https://doi.org/10.3189/S0022143000002276>
- Peña, H., Escobar, F., & Vidal, F. (1987). Estimación de tasas de derretimiento de nieve. *VII Congreso Nacional Sociedad Chilena de Ingeniería Hidráulica*.
- Rabatel, A., Castebrunet, H., Favier, V., Nicholson, L., & Kinnard, C. (2011). Glacier changes in the Pascua-Lama region, Chilean Andes (29° S): recent mass balance and 50 yr surface area variations. *The Cryosphere*, 5(4), 1029–1041. <https://doi.org/10.5194/tc-5-1029-2011>
- Rabatel, A., Letréguilly, A., Dedieu, J. P., & Eckert, N. (2013). Changes in glacier equilibrium-line altitude in the western Alps from 1984 to 2010: Evaluation by remote sensing and modeling of the morphotopographic and climate controls. *Cryosphere*, 7(5), 1455–1471. <https://doi.org/10.5194/tc-7-1455-2013>
- Radić, V., & Hock, R. (2011). Regionally differentiated contribution of mountain glaciers and ice caps to future sea-level rise. *Nature Geoscience*, 4(2), 91–94. <https://doi.org/10.1038/ngeo1052>
- Ragetli, S., & Pellicciotti, F. (2012). Calibration of a physically based, spatially distributed hydrological model in a glacierized basin: On the use of knowledge from glaciometeorological processes to constrain model parameters. *Water Resources Research*, 48(3), 1–20. <https://doi.org/10.1029/2011WR010559>
- Ragetli, S., Pellicciotti, F., Bordoy, R., & Immerzeel, W. W. (2013). Sources of uncertainty in modeling the glaciohydrological response of a Karakoram watershed to climate change. *Water Resources Research*, 49(9), 6048–6066. <https://doi.org/10.1002/wrcr.20450>
- RGI Consortium. (2017). *Randolph Glacier Inventory – A Dataset of Global Glacier Outlines: Version 6.0: Technical Report, Global Land Ice Measurements from Space*. Retrieved from [https://www.glims.org/RGI/00\\_rgi60\\_TechnicalNote.pdf](https://www.glims.org/RGI/00_rgi60_TechnicalNote.pdf)
- Rivera, A., & Bown, F. (2013). Recent glacier variations on active ice capped volcanoes in the southern volcanic zone (37°-46°s), Chilean andes. *Journal of South American Earth Sciences*, 45, 345–356. <https://doi.org/10.1016/j.jsames.2013.02.004>
- Rivera, A., Casassa, G., Acuña, C., & Lange, H. (2000). Variaciones recientes de glaciares en Chile. *Investigaciones Geográficas*, 34, 29. <https://doi.org/10.5354/0719-5370.2000.27709>
- Rivera, A., Casassa, G., Bamber, J., & Kääb, A. (2005). Ice-elevation changes of Glaciar Chico, southern Patagonia, using ASTER DEMs, aerial photographs and GPS data. *Journal of Glaciology*, 51(172), 105–112. <https://doi.org/10.3189/172756505781829557>
- Rivera, A., Koppes, M., Bravo, C., & Aravena, J. C. (2012). Little Ice Age advance and retreat of Glaciar Jorge Montt, Chilean Patagonia. *Climate of the Past*, 8(2), 403–414. <https://doi.org/10.5194/cp-8-403-2012>
- Sagredo, E. A., & Lowell, T. V. (2012). Climatology of Andean glaciers: A framework to understand glacier response to climate change. *Global and Planetary Change*, 86–87(April 2012), 101–109. <https://doi.org/10.1016/j.gloplacha.2012.02.010>

- Sakai, A., & Fujita, K. (2017). Contrasting glacier responses to recent climate change in high-mountain Asia. *Scientific Reports*, 7(1), 1–8. <https://doi.org/10.1038/s41598-017-14256-5>
- Schaefer, M., Fonseca-Gallardo, D., Farías-Barahona, D., & Casassa, G. (2020). Surface energy fluxes on Chilean glaciers: measurements and models. *The Cryosphere*, 14(8), 2545–2565. <https://doi.org/10.5194/tc-14-2545-2020>
- Schaefer, M., Rodriguez, J. L., Scheiter, M., & Casassa, G. (2017). Climate and surface mass balance of Mocho Glacier, Chilean Lake District, 40°S. *Journal of Glaciology*, 63(238), 218–228. <https://doi.org/10.1017/jog.2016.129>
- Schumacher, V., Justino, F., Fernández, A., Meseguer-Ruiz, O., Sarricolea, P., Comin, A., Peroni Venancio, L., & Althoff, D. (2020). Comparison between observations and gridded data sets over complex terrain in the Chilean Andes: Precipitation and temperature. *International Journal of Climatology*, 40(12), 5266–5288. <https://doi.org/10.1002/joc.6518>
- Seehaus, T., Malz, P., Sommer, C., Lippl, S., Cochachin, A., & Braun, M. (2019). Changes of the tropical glaciers throughout Peru between 2000 and 2016 - Mass balance and area fluctuations. *Cryosphere*, 13(10), 2537–2556. <https://doi.org/10.5194/tc-13-2537-2019>
- Sevestre, H., & Benn, D. I. (2015). Climatic and geometric controls on the global distribution of surge-type glaciers: Implications for a unifying model of surging. *Journal of Glaciology*, 61(228), 646–662. <https://doi.org/10.3189/2015JoG14J136>
- Shaw, T. E., Caro, A., Mendoza, P., Ayala, Á., Pellicciotti, F., Gascoin, S., & McPhee, J. (2020). The Utility of Optical Satellite Winter Snow Depths for Initializing a Glacio-Hydrological Model of a High-Elevation, Andean Catchment. *Water Resources Research*, 56(8), 1–19. <https://doi.org/10.1029/2020WR027188>
- Wang, R., Liu, S., Shangguan, D., Radić, V., & Zhang, Y. (2019). Spatial heterogeneity in glacier mass-balance sensitivity across High Mountain Asia. *Water (Switzerland)*, 11(4), 1–21. <https://doi.org/10.3390/w11040776>
- Warren, C. R. (1993). Rapid Recent Fluctuations of the Calving San Rafael Glacier , Chilean Patagonia : Climatic or Non-Climatic ? *Geografiska Annaler*, 75(3), 111–125. <https://doi.org/10.2307/521029>
- Weidemann, S. S., Sauter, T., Malz, P., Jaña, R., Arigony-Neto, J., Casassa, G., & Schneider, C. (2018). Glacier mass changes of lake-terminating grey and tyndall glaciers at the southern patagonia icefield derived from geodetic observations and energy and mass balance modeling. *Frontiers in Earth Science*, 6, 1–16. <https://doi.org/10.3389/feart.2018.00081>
- Winchester, V., & Harrison, S. (1996). Recent Oscillations of the San Quintin and San Rafael Glaciers , Patagonian Chile. *Geografiska Annaler*, 78(1), 35–49. <https://doi.org/10.1080/04353676.1996.11880450>
- Zemp, M., Huss, M., Thibert, E., Eckert, N., McNabb, R., Huber, J., Barandun, M., Machguth, H., Nussbaumer, S. U., Gärtner-Roer, I., Thomson, L., Paul, F., Maussion, F., Kutuzov, S., & Cogley, J. G. (2019). Global glacier mass changes and their contributions to sea-level rise from 1961 to 2016. *Nature*, 568(7752), 382–386. <https://doi.org/10.1038/s41586-019-1071-0>

**Supplementary information**

Supplementary I. Monthly climatic values between 1980-2019.

Glacier cluster	Monthly climatic values 1980-2019											
	Jan	Feb	Mar	Apr	May	Jun	Jul	Aug	Sep	Oct	Nov	Dec
<b>Precipitation [mm/month]</b>												
1	62.8	69.7	44.7	1.4	0.1	0.3	2.1	0.1	1.6	0.6	10.2	27.3
2	8.2	19.0	10.6	3.8	22.2	22.8	26.1	18.9	8.8	6.7	4.2	5.7
3	10.4	17.9	19.6	19.4	64.0	52.1	57.6	57.5	31.8	28.2	11.1	9.4
4	6.1	10.6	14.8	22.9	77.0	71.2	60.8	69.9	32.8	32.4	11.0	6.4
5	7.9	13.5	17.8	33.9	93.0	103.7	83.7	91.4	39.2	35.8	17.6	9.2
6	68.1	77.7	108.4	145.7	196.6	217.5	199.2	196.8	125.4	99.7	103.4	91.2
7	53.9	66.4	99.4	127.4	153.0	177.9	161.0	159.4	101.6	81.8	89.4	76.9
8	59.2	69.8	100.5	129.4	159.9	181.6	163.2	163.6	104.9	86.2	92.1	79.8
9	61.2	72.0	96.2	105.3	96.3	105.0	84.5	95.0	63.8	73.0	82.7	67.1
10	72.7	85.2	101.3	101.8	79.7	87.2	78.4	84.7	59.1	71.3	81.1	76.4
11	165.4	174.9	198.9	204.4	174.3	164.6	161.5	170.9	124.5	166.3	167.7	160.2
12	319.4	332.0	371.6	349.3	286.0	250.1	295.5	307.2	210.4	305.9	301.6	307.8
13	126.9	132.6	139.0	134.2	106.4	116.3	118.2	110.2	93.9	100.8	106.9	124.1
<b>Temperature [°C/month]</b>												
1	4.7	4.4	4.1	2.8	0.2	-2.3	-2.5	-1.7	0.6	2.1	3.5	4.6
2	3.1	2.6	1.6	-0.5	-2.6	-4.9	-5.3	-4.7	-3.5	-2.3	0.2	2.0
3	-0.4	-1.0	-1.9	-4.3	-7.1	-10.4	-10.8	-10.1	-8.9	-7.1	-4.3	-1.7
4	4.5	3.8	2.6	-0.1	-3.5	-7.1	-7.4	-6.6	-5.4	-3.1	-0.1	2.9
5	9.1	8.4	6.8	3.8	0.4	-2.7	-3.0	-2.2	-0.8	1.7	4.6	7.4
6	13.4	13.0	11.0	7.9	5.3	3.2	2.3	3.5	5.3	7.7	9.7	11.9
7	10.2	9.9	7.9	4.7	2.1	-0.1	-1.0	0.3	2.1	4.4	6.6	8.7
8	11.5	11.1	9.2	6.1	3.4	1.3	0.4	1.6	3.5	5.9	7.9	10.1
9	8.9	8.6	6.8	4.1	1.4	-0.8	-1.2	-0.4	1.6	3.9	5.7	7.8
10	6.7	6.4	4.9	2.3	-0.3	-2.3	-2.5	-2.0	-0.1	2.1	3.6	5.6
11	9.7	9.5	8.1	5.9	3.4	1.7	1.5	1.9	3.7	5.6	6.9	8.7
12	9.5	9.5	8.1	6.2	4.0	2.7	2.5	2.6	4.1	5.8	6.8	8.6
13	8.0	7.8	6.8	4.6	2.5	0.8	0.8	1.2	2.8	4.6	5.5	7.2

Glacier cluster	Monthly climatic values 1980-2019											
	Jan	Feb	Mar	Apr	May	Jun	Jul	Aug	Sep	Oct	Nov	Dec
<b>Solar radiation [W/m2/month]</b>												
1	224.2	199.5	224.4	210.1	182.6	175.5	179.6	206.7	233.3	251.1	258.7	248.4
2	307.9	275.3	258.2	204.6	136.4	112.7	119.8	156.5	216.3	275.2	311.8	334.5
3	284.9	251.1	223.5	157.4	103.5	93.4	100.8	131.2	173.5	228.7	270.1	297.2
4	291.4	264.5	223.9	157.5	100.3	84.4	94.3	123.9	167.9	221.6	268.3	300.5
5	294.2	263.1	216.6	154.4	99.0	81.0	91.4	119.9	168.0	217.9	266.1	297.2
6	232.3	206.3	146.4	95.7	61.0	40.8	48.6	76.0	107.8	156.6	194.1	221.8
7	208.7	185.0	130.1	82.6	56.2	34.0	41.6	64.7	91.6	132.7	162.8	194.8
8	218.4	193.3	136.3	87.3	56.6	35.6	43.3	68.2	97.1	143.1	175.8	206.4
9	185.9	159.6	110.6	69.1	44.6	27.9	34.8	55.6	82.7	127.8	158.2	181.6
10	173.6	148.8	102.2	62.2	40.4	26.2	32.1	53.0	79.0	121.7	151.1	172.9
11	162.9	143.2	98.1	64.8	43.1	29.2	34.1	59.6	82.6	123.3	150.5	167.0
12	154.4	137.4	93.6	61.1	40.1	24.1	27.9	51.6	76.8	117.4	147.4	160.9
13	151.6	131.6	87.2	51.2	31.8	18.6	22.8	43.8	70.6	114.5	149.5	160.1

Source: self-made.